Developing an integrated 3D-printed façade with complex geometries for active temperature control

Sarakinioti, Valentini; Turrin, Michela; Konstantinou, Thaleia; Tenpierik, Martin; Knaack, Ulrich

DOI
10.1016/j.mtcomm.2018.02.027

Publication date
2018

Document Version
Accepted author manuscript

Published in
Materials Today Communications

Elsevier 3D Printing Grand Challenge
Title: Developing an integrated 3D-printed façade with complex geometries for active temperature control

Authors: Msc.Ing. Maria Valentini Sarakinioti[1],dr.M. Arch Michela Turrin[2], dr. Ing. Msc.Thaleia Konstantinou[3], Dr.Ir. Martin Tenpierik[4], prof.dr.ing. Ulrich Knaack[5]

Keywords: Façade, AM, FDM technology, Plastic filament, movable heat storage, thermal insulation

1. Introduction

Additive manufacturing (AM) provides great freedom of form, enhancing the freedom of designers and engineers in creating complex designs. This design freedom refers to four categories: shape complexity, hierarchical complexity, material complexity and functional complexity (Yang & Zhao, 2015). Because the freedom in geometric complexity applies also to the inner part of the products manufactured with additive processes, it is possible to customize inner geometries to integrate multi-functionalities. For example, operational mechanisms and embedded components can be fabricated directly (Yang & Zhao, 2015). The research presented here focuses on the freedom of form as main advantage of AM (Strauss & Knaack, 2016), applied to facades in the building industry. The façade is one of the most challenging parts of a building, being a multifunctional component that controls the indoor environment of a building (Strauss & Knaack, 2016). Moreover, the growing demand for low energy consumption and a raised sense of comfort have given the façade a new important role in the overall building concept. Little research has been conducted into the load-bearing capacities and/or other essential qualities of AM products for the building industry, such as durability, water vapor diffusion resistance, thermal conductivity or fire-resistance. This is most probably due to the way in which constructions are organized today, as a combination of materials each of which has its specific properties (Labonnote, Rønnquist, Manum, & Rüther, 2016). AM in the façade industry opens new major potentials, but also requires relevant research to be conducted.

In this context, the present research focused on the potentials of AM for an adaptive facade system that optimizes thermal performances according to different environmental conditions. The general objective was to prove that AM enables the creation of mono-material façade components that integrate multiple functions. The specific objective was to create a plastic façade panel that can regulate the temperature inside a building throughout the whole year, focusing on the thermal properties of porous structures and the heat storage capacity of liquids. The final product is a proof of concept for an adaptive façade panel that controls the heat exchange between the indoor and the outdoor environment by integrating geometries for thermal insulation and heat storage, while guaranteeing structural strength.

This paper presents the design and production of the façade panel. First the composition of the façade panel is explained, as well as the parameters that led to the design choices. Then four research phases are presented. In the first one, samples were designed, and 3D printed based on symmetrical cellular structures. In the second phase, samples were designed, and 3D printed based on elongated and asymmetrical structures; a broad range of heat flux and temperature measurements were conducted. In the third phase, channels for water circulation were designed, 3D-printed and tested for water tightness. Finally, the most promising design principles were scaled-up into larger prototypes. At last, conclusions are discussed.

The 3d printing process that was selected was Fused Deposition Modelling. FDM technology and plastic filament are easily accessible to anyone who wants to 3d print. In addition, plastic is relatively lightweight, has low thermal conductivity and is recyclable. Transparent PETG was chosen due to higher solar transmittance for the external layer. Moreover, PETG has higher stiffness and strength than PLA. Three different nozzle sizes were used to compare the quality and speed of the printing process: 0.4 mm, 0.8 mm, and 1.2 mm. The slicing settings were adjusted to find the optimum speed and quality of print. Multiple samples were produced for the different parts of the façade with variation in different parameters such as: layer height, infill percentage, speed, extrusion width and

[1,2,3,4,5] TU Delft, Faculty of Architecture and the Built Environment, department of Architectural Engineering & Technology, Delft

temperature. The results received from thermal simulations showed what the potentials of this proof of concept are for heating and cooling in different climates throughout the year. The most promising scenario was selected for further development.

2. Design configurations: The insulation part

The façade panel has two main functions: thermal insulation and movable liquid heat storage. The insulation is placed in the core of the façade panel and consists of cavities that integrate air. The dimension of a cell in the direction of the heat transfer based on theoretical models needs to be 15mm max to prevent the development of convention inside the cells.

Phase 1: Polyhedra

The first phase of this research focused on closed cellular structures that have relatively good thermal performance (Ashby, 2006). First, the Waire Phelan polyhedral configuration was chosen to be tested for its thermal properties. Physicists Dennis Waire and Robert Phelan identified a new type of cell for regular foams that has the lowest surface area of any known monodisperse structure (Weaire, 1997).This capacity creates potentials for cellular structures that have relatively low ratio of solid to gas. Previous investigation in the cells of 10mm showed that they have relatively low thermal conductivity,0.044 W/(m·K) (Sarakinioti, 2016). The external part of the façade was designed to have cells of 30 mm size that are connected to create channels that could integrate also the heat storage based on circulation of liquids. A sample with this configuration, with one input and output for the water was designed and 3d printed. The results showed that the polyhedra require relatively large printing time or have high risks of vibrations during printing due to the sharp edges when the printing speed increases. Moreover, additional support was needed underneath the horizontal surfaces of the polyhedra. Thirdly, regarding the structural performance, the strength of the polyhedra exceeded the requirements, and, hence, large cavities in the core of the panel are generated to reduce the used material. However, in large cavities heat transfer by convention increases, which reduces the insulation capacity of the panel. Therefore, the polyhedra resulted to be sub-optimal for at least one of the considered criteria and were discarded.

Phase 2: Elongated cells

In this phase, the goal was to design configurations able to reduce the material (and thus having higher porosity), and the printing time and at the same time to increase the thermal resistance. The cells were stretched in all directions except for the direction of the heat transfer (we kept it between 10-20mm to minimise convective heat transfer). Samples 2-5(Table1) where tested for their thermal conductivity. In order to calculate the ratio of solid to gas, we calculated the volume of the solid part of the sample and the volume of the void(the part that has air).Then the V_s(volume of the solid part) was divided with the V_g(gas part).(Vs/Vg)This process was followed for all the samples and the results were compared in the end to conclude which sample is the most lightweight and therefore has the good potentials for low thermal conductivity.

Table 1 Data of the polyhedra and the elongated cells

	Physical properties/printing settings											Results of thermal properties/printing time	
	Nr	Cell length	Dimensions mm (height, lenght, thickness)	Material	Nozzle size mm	Wall thick. mm	Infill	Mass kg	Speed mm/s	Layer height mm	Ratio of solid to gas(Vs/Vg)	λ thermal conductivity W/(m·K)	Time h
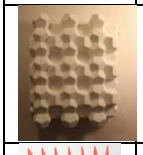	1		150x150x36	PLA	0.4	1.6,3.2	10%	0.320	21	0.1	-	-	69
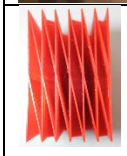	2	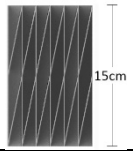	180x180x100	PETG clr.	0.4	1.2	0%	0.533	28	0.1	0.2	0.101	40

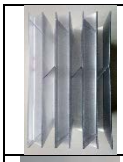	3	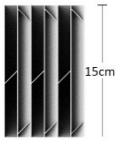	200x200 x100	PETG tr.	0.4	0.8	0%	0.286	28	0.1	0.08	0.094	35
	4	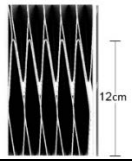	180x180 x100	PETG tr.	0.4	1.2	0%	0.417	28	0.1	0.23	0.104	24
	5	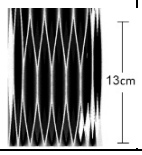	200x200 x100	PETG tr.	0.4	1.2	0%	0.693	28	0.1	0.23	0.109	30

Tests of thermal conductivity properties

For testing the effective thermal conductivity of the samples, a chamber of 1 m^3 made of polystyrene panels was built and a hole of 20cmx20cm was created in one side of the box to place the samples. A lamp was placed inside the box to increase the temperature and create a difference with the temperature in the environment. The tests took place during the summer months. In one typical summer day the mean temperature of the office was 28.7^{o}C. In that day the temperature inside the box was 54^{o}C and outside 28.7^{o}C. The difference was 25. 3^{o}C.The temperature difference to have a reliable conclusion for the thermal conductivity of the sample needs to be at least 20^{o}C.

During a test, the heat flux through both surfaces of the sample (with Hukseflux HFP01 heat flux plates) and the temperature inside the box, outside the box and on both surfaces of the sample (with thermocouples) were measured. The sensors were connected to data acquisition modules of Eltek (Gen II system). Each measurement lasted 7 hours to ensure a steady-state measurement condition. The samples had a size of 18x18x10 cm^3 or 20x20x10 cm^3.

3. Design configurations: The heat storage

The heat storage is a water-based liquid that is placed in the façade when and where needed each time of the year. It is either stored in one of the two external layers of the façade which consist of channels or in a water tank in the centre of the facade. To control the movement of the liquid through the overall system the two external layers integrate two reversible pumps for the water circulation. In a cooling situation, the water is placed inside during the daytime to absorb the heat gain and during the night is pumped outside to discharge to the cool night sky (Figure 2a). In a heating season the water is placed outside in the daytime to absorb the heat gain from the solar radiation and during the night is pumped inside to realise the heat. (Figure 2b)

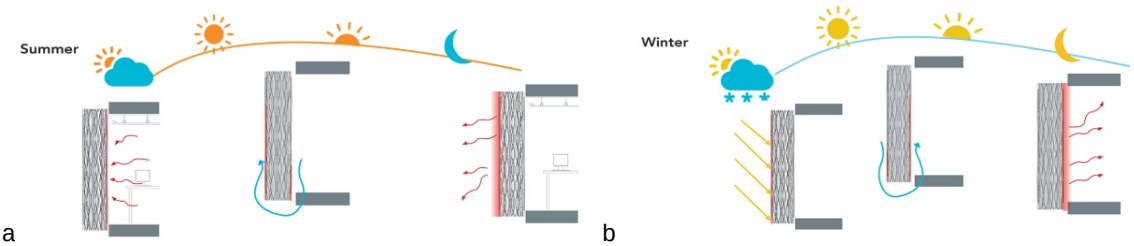

a b

Figure 1 Water circulation in a cooling season (a), in a heating season (b) (source:M.de Klijn, V. Sarakinioti)

The design of the external layer was inspired by natural configurations that transfer fluids such as blood vessels, veins in leaves and 3d bionic structures. Different configurations were tested. The first calculations for the heat storage capacity showed that the external layer needed to be 15mm.The final design integrates channels that have a diameter which gradually decreases.

	Nr.	Size of the channels	Dimensions mm((height, lenght, thickness)	Material	Nozzle size mm	Wall thick. mm	Infill	Layer height mm	Speed mm/s	Mass kg	Time (h)
	6	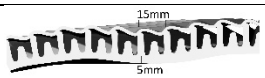	74x210x30	PETG tr	1.2	4.8	30%	0.6	21	0.125	4
	7	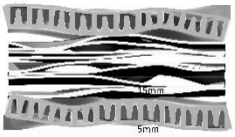	300x210x100	PETG tr	1.2	2.4	0%	0.6	21	1.5	66
	8	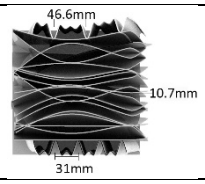	170x200x200	PETG tr	1.2	1.2	0%	0.8	21	0.819	12
	9		140x120x15	PETG tr	1.2	2.6	0%	0.8	21	0.135	1
	10	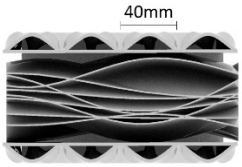	660x200x100	PETG tr	1.2	2.6	0%	0.8	21	1.5	24

Table 2Data of the samples for external layer (channels for heat storage)

Samples 6 and 7 have channels of 15 mm diameter that transform to smaller channels of 5 mm diameter each. Additionally, sample 6 has an irregular external surface whereas sample 7 has a flat external surface. Sample 7 integrates the thermal insulation and the channels for heat storage and was tested for water tightness. Sample 8 is a fragment of a next design; the external layer has a single wall and the diameter of the channels start from 5 mm and gradually becomes 15 mm diameter. Sample 9 is a fragment of the external layer of the final design; the external surface has two walls with total thickness of 2.4 mm and channels of maximum 40 mm diameter and minimum 20 mm diameter. Sample 10 is the final working prototype which was tested for water tightness.

External layer surface properties

Samples 7 and 10 were also tested for water tightness. The equipment used was a water pump (Eheim universele pomp/300lt/h 1.7m kabel) and a hose (diam.10mm) that connects the input of the sample with the output of the pump. Sample 7 has a curved shape and the top part has an inclination of less than 45^{o}, which challenged the adhesion of the deposited layers leading to evident micro-holes. The next step was to apply Acrylic based coating. The result was not the expected and the leaking started to occur. Next step was to design smaller samples and test(sample9) and finally sample 10, which did not have design faults, however the surface had micro-holes in between layers, expectantly caused by discontinuities and high-speed in the printing process. An epoxy coating (EpoxAcast690p Epoxacast 690 clear) was applied both on the inside of the channels and on the external surface of the component to ensure water tightness.

4. Large scale prototype

According to the dimensions of the big printer the large prototype was constructed in two pieces that are connected vertically with an interlocking system.

Sample 11 is a simplified version of the original design and is double curved. It has fewer surfaces in comparison with the original model and simplified external layer. In addition, it is the low part of the façade panel. Some aspects challenged the printing process. The channels of the external layer had

one single wall. Because the channels had small thickness the extruder could apply pressure on them and gradually cause a displacement and deformation at these parts. Every surface from the insulation part was separately connected to the print bed with a narrow base. In that case, during the printing process the vibrations to the model increased possibilities of deformation.

In Sample 12 the diameter of the channels was increased 20mm diameter for the small channels and 40mm diameter for the big channels. In that case the printing time was decreased and therefore the risk for failure. Moreover, a second wall in the channels was inserted to make them stiffer with total thickness of 2.4mm. A single base for all the parts of the object was designed. The large panel had a rectangular shape. The printing process of the large component was completed successfully; expect the small cavities in the surface at the part of the transition from large to small channels. The design in this part was slightly adjusted and printed in smaller samples. Moreover, some settings in the slicing program changed and tested to conclude in the final design and settings for the slicing process. The top part of the large prototype, was 3d printed with a cavity in its core. Since it is a prototype of demonstration reduction of the material and printing time was required. The two models were interlocked vertically and consist of a free-standing component. (13)

Table 3 Data for samples of large prototype

		Physical properties/printing settings									
	Nr.	Section of the model	Dimensions mm((height, lenght, thickness))	Material	Nozzle size mm	Wall thick. mm	Infill	Layer height	Speed mm/s	Mass kg	Time h
	11	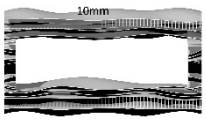	300x300x550	PETG tr	1.2	1.2	0%	0.8	21	-	Failed model
	12	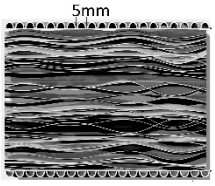	750x500x360	PETG tr	1.2	1.2 cells, 2.4 channels	0%	0.8	21	20	296
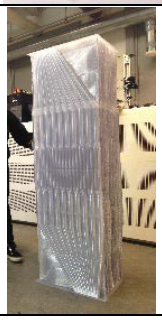	13 Top part		750x500x360	PETG tr	1.2	1.2	0%	0.8	21	15	216

5. Conclusion

Integrating multiple functions for optimizing thermal performances and creating mono material structures is possible with 3d printing technology. For the insulation, it is proved that low thermal conductivity is achievable by controlling the size of the cells and the geometry of the cells. The material also is a major parameter for the low thermal conductivity. The range for the different configurations was $0.09<\lambda<0.1$ W/(m·K) whereas in conventional insulation materials the range is approximately $0.02<\lambda<0.14$ W/(m·K) where 0.02 W/(m·K) is for silica aerogel and 0.14 W/(m·K) is for timber. The printing time between the different configurations is decreased when the cells change from sharp edges to curvy edges, because the extruder follows a continuous path while printing. With thickness of 33cm insulation the U value is 0.30W/(m^2·K). In addition, the configurations selected for the heat storage have potentials for minimal pressure drop and uniform flow. Moreover, the tests

showed challenges for water-tightness, at this stage leading to post printing process on the external layer. The final working prototype (Sample 10) was connected with a pump and a hose and could fill one layer. Large scale 3d printing with a 1.2mm nozzle highlighted the time-consuming production process. The project is at the proof-of-concept phase, which suggests that further research is required, on several aspects. First direction for the further research will be the improvement of the thermal conductivity and that requires a more systematic process in the design of the insulation part with an optimization process for reducing the material and the thermal conductivity. The size of the cells and the geometry can be further investigated to achieve higher thermal resistance. Moreover, investigation on the material by using polymers that have low thermal conductivity value. Second direction will be to improve the water tightness and overcome the demand to use post processing with coatings in the 3d printed part. Moreover, optimize the size of the channels to improve the drop of the pressure of the flow. In addition, further investigation needs to be done for the feasibility of the production for large scale components regarding time and costs. Finally, further investigation needs to be done for the structural tests especially for the durability and the deformations in extreme thermal conditions.

6. Acknowledgment

This research proposal was funded from 4TU Federation and co funded from TU Delft and TU Eindhoven for the development this project (2016-2017). This project is the result of the collaboration of researchers from TU Delft and TU Eindhoven. From TU Eindhoven researchers MSc Marie de Klijn, ir. Roel Loonen, prof.dr.ir. Jan Hensen and student R.N.P Woensel from the department of the Built Environment and section of building physics and services. Ir Arno Pronk, prof.dr.-ing. Patrick Teuffel and students Eline Dolkemade, Arthur van Lier, Rens Vorstermans, from the section of structural design. From TU Delft researchers ir Paul de Ruiter, March Milou Teeling, MSc.Mark van Erk from the chair of design informatics. The production of the large-scale prototypes and the samples of the thermal tests was developed in KIWI solutions by Dick Vlasblom.

7. References

Ashby, M. (2006). The properties of foams and lattices. *Philosophical Transactions of the Royal Society of London A: Mathematical, Physical and Engineering Sciences, 364*(1838), 15-30.

Labonnote, N., Rønnquist, A., Manum, B., & Rüther, P. (2016). Additive construction: State-of-the-art, challenges and opportunities. *Automation in Construction, 72, Part 3*, 347-366. doi:https://doi.org/10.1016/j.autcon.2016.08.026

Sarakinioti, M. (2016). The spongy skin: The potentials of AM methods in cellular structures.

Strauss, H., & Knaack, U. (2016). Additive Manufacturing for Future Facades. *2016, 3*(3-4), 11. doi:10.7480/jfde.2015.3-4.875

Weaire, D. (1997). *The Kelvin Problem*: CRC Press.

Yang, S., & Zhao, Y. F. (2015). Additive manufacturing-enabled design theory and methodology: a critical review. *The International Journal of Advanced Manufacturing Technology, 80*(1), 327-342. doi:10.1007/s00170-015-6994-b